

the Met markers pattern, the major Fe<sup>2+</sup> cleavage occurs between Met<sup>466</sup> and Met<sup>400</sup> (Fig. 5, lane 7). At the same time, the major cleavage product co-migrates with the Cys<sup>454</sup> marker (Fig. 5, lane 6; and Fig. 1). As can be seen from Fig. 1, Cys<sup>454</sup> flanks the evolutionarily conserved region D of the β' polypeptide containing the NADFDGD (13) sequence. Thus, the major Fe<sup>2+</sup> cleavage occurs next to this motif.

These results strongly suggest that the aspartates of the NADFDGD sequence are involved in chelating the Mg<sup>2+</sup> ion in the active center of RNAP (14). In DNA polymerase I and human immunodeficiency virus reverse transcriptase, the acidic residues that perform this function are located at the base of the cleft in the three-dimensional (3D) structure, the site where the catalytic reaction is believed to take place (1). A similar cleft has been observed in low-resolution contours of RNAP from *E. coli* (15) and yeast RNAP II (16) and RNAP I (17). Thus, in these large multisubunit RNAPs, the NADFDGD motif is probably located in the base of the cleft, where it forms the crucial element of the active center. Further evidence for the functional importance of the NADFDGD motif has come from extensive mutagenesis performed on yeast RNA polymerase III (18). Previous cross-linking experiments have implicated other sites in the active center of *E. coli* RNAP. Segments 515 to 660 and 1091 to 1107 in β and 330 to 366 and 932 to 1020 in β' are facing the 3' terminus of RNA in the catalytic pocket (19, 20). Lys<sup>1065</sup> and His<sup>1237</sup> of the β subunit are located on the 5' side facing the priming nucleoside triphosphate (21, 22). The Rif-binding site is located upstream of the 5' face along the exit path of the transcript (12, 23). Our present results indicate that all these sites are juxtaposed to the NADFDGD motif in the 3D structure of RNAP and probably line the surface of the cleft where the active center is located.

REFERENCES AND NOTES

1. C. M. Joyce and T. A. Steitz, *Annu. Rev. Biochem.* **63**, 777 (1994).
2. W.-C. Suh, S. Leirimo, T. Record Jr., *Biochemistry* **31**, 7815 (1992).
3. M. A. Price and T. D. Tullius, *Methods Enzymol.* **212**, 194 (1992).
4. C. H. Wei, W. Y. Chou, S. M. Huang, C. C. Lin, G. G. Chang, *Biochemistry* **33**, 7931 (1994).
5. C. H. Wei, W. Y. Chou, G. G. Chang, *ibid.* **34**, 7949 (1995).
6. W. Y. Chou, W. P. Tsai, C. C. Lin, G. G. Chang, *J. Biol. Chem.* **270**, 25935 (1995).
7. J. M. Farber and R. L. Levine, *ibid.* **261**, 4574 (1986).
8. N. Eitner *et al.*, *Biochemistry* **34**, 22 (1995).
9. S. Borukhov and A. Goldfarb, *Protein Expr. Purif.* **4**, 503 (1993).
10. D. G. Knorre, O. S. Fedorova, E. I. Frolova, *Russ. Chem. Rev.* **62**, 65 (1993).
11. A. A. Mustaev *et al.*, *Proc. Natl. Acad. Sci. U.S.A.* **91**, 12036 (1994).

12. V. Markovtsov, in preparation.
13. Abbreviations for the amino acid residues are as follows: A, Ala; C, Cys; D, Asp; E, Glu; F, Phe; G, Gly; H, His; I, Ile; K, Lys; L, Leu; M, Met; N, Asn; P, Pro; Q, Gln; R, Arg; S, Ser; T, Thr; V, Val; W, Trp; and Y, Tyr.
14. Mg<sup>2+</sup> is also required for promoter opening [W.-C. Suh, W. Ross, T. Record Jr., *Science* **259**, 358 (1993)]. Because the DDD mutant opens the promoter, the Mg<sup>2+</sup> ion involved in the opening must be different from the one held by the substituted aspartates in the active center.
15. S. A. Darst, E. W. Kubalek, R. D. Kornberg, *Nature* **340**, 730 (1989).
16. S. A. Darst, A. M. Edwards, E. W. Kubalek, R. D. Kornberg, *Cell* **66**, 121 (1991).
17. P. Schultz, H. Celia, M. Riva, A. Sentenac, P. Oudet, *EMBO J.* **12**, 2607 (1993).
18. G. Dieci *et al.*, *ibid.* **14**, 3766 (1995).
19. V. Markovtsov, A. Mustaev, A. Goldfarb, *Proc. Natl. Acad. Sci. U.S.A.* **93**, 3221 (1996).

20. S. Borukhov, J. Lee, A. Goldfarb, *J. Biol. Chem.* **266**, 23932 (1991).
21. M. A. Grachev *et al.*, *Eur. J. Biochem.* **180**, 577 (1989).
22. A. Mustaev *et al.*, *J. Biol. Chem.* **266**, 23927 (1991).
23. K. Severinov *et al.*, *ibid.* **270**, 29428 (1995).
24. E. Martin, thesis, Institute of Molecular Genetics, Russian Academy of Science, Moscow (1992).
25. E. Zaychikov, L. Denissova, H. Heumann, *Proc. Natl. Acad. Sci. U.S.A.* **92**, 1739 (1994).
26. M. Kashlev, *et al.*, *Gene* **130**, 9 (1993).
27. E. Nudler, A. Goldfarb, M. Kashlev, *Science* **265**, 793 (1994).
28. Supported by a grant from NIH (to A.G.), by a grant from Deutsche Forschung-Gemeinschaft (to H.H.), and by a Fogarty International Research Collaboration Award grant (to A.G. and E.Z.). We are grateful to S. Borukhov and E. Nudler for comments.

20 February 1996; accepted 17 April 1996

## Prevention of Islet Allograft Rejection with Engineered Myoblasts Expressing FasL in Mice

Henry T. Lau,\* Ming Yu, Adriano Fontana, Christian J. Stoeckert Jr.

Allogeneic transplantation of islets of Langerhans was facilitated by the cotransplantation of syngeneic myoblasts genetically engineered to express the Fas ligand (FasL). Composite grafting of allogeneic islets with syngeneic myoblasts expressing FasL protected the islet graft from immune rejection and maintained normoglycemia for more than 80 days in mice with streptozotocin-induced diabetes. Graft survival was not prolonged with composite grafts of unmodified myoblasts or Fas-expressing myoblasts. Islet allografts transplanted separately from FasL-expressing myoblasts into the contralateral kidney were rejected, as were similarly transplanted third-party thyroid allografts. Thus, the FasL signal provided site- and immune-specific protection of islet allografts.

Immunological rejection of pancreatic islet allografts remains a major obstacle toward the application of such transplants in the treatment of diabetes mellitus. Interactions of Fas with its ligand (FasL) are thought to play a major role in the maintenance of immunological homeostasis and peripheral tolerance (1). We investigated whether provision of the FasL signal by transfected syngeneic myoblasts within the local environment of an islet allograft can deliver a death signal to infiltrating allo-activated T cells that express Fas (2) and thereby protect the islet allograft from rejection. This approach could permit the use of plasmid-based gene delivery into carrier cells such as myoblasts and make unnecessary the direct

transfection of islet allografts.

A muscle cell-based delivery system that is effective in the delivery of recombinant molecules (3) was used. Primary myoblasts from adult C57BL/6 (B6) (H-2<sup>b</sup>) mice were transfected with the plasmid BCMGS Neo-FasL (4), and G418-resistant colonies were pooled and designated BfasL. These cells were analyzed for FasL expression by fluorescence-activated cell sorting (FACS) with the fusion protein Fas-Fc, which is the specific counterreceptor for FasL. The BfasL cells were positive for FasL, whereas nontransfected B6 myoblasts (designated B6a) showed only background staining (Fig. 1A). The ability of B6 myoblasts to express recombinant FasL and to survive is consistent with the observation that muscle cells do not express Fas (5). The Fas<sup>+</sup> murine lymphoma cell line YAC-1 was used as a target in a cytotoxicity assay (6) to ascertain whether the FasL-expressing myoblasts could deliver an apoptotic signal to Fas-bearing cells. BfasL myoblasts cocultured with YAC-1 cells for 12 hours induced YAC-1 cell death (Fig. 1B) and DNA fragmentation (Fig. 1C), consistent with death by apoptosis (7), whereas coculture with

H. T. Lau and M. Yu, Department of Pediatric Surgery, Children's Hospital of Philadelphia, University of Pennsylvania, Philadelphia, PA 19104, USA  
 A. Fontana, Department of Internal Medicine, Section of Clinical Immunology, University Hospital of Zurich, Haldeliweg 4, CH-8044 Zurich, Switzerland.  
 C. J. Stoeckert Jr., Department of Hematology, Abramson Center, Children's Hospital of Philadelphia, Philadelphia, PA 19104, USA.

\*To whom correspondence should be addressed at Department of Pediatric Surgery, Johns Hopkins Hospital, Baltimore, MD 21287, USA.

B6a myoblasts had no effect.

Transplantation experiments were performed with composite grafts of genetically engineered myoblasts and unmanipulated allogeneic islets to test whether expression of FasL in the vicinity of the islet allograft conferred protection from rejection. Diabetic B6 mice were used as recipients because they are syngeneic to Bfasl muscle cells. The composite grafts were transplanted under the kidney capsule (8). Control

animals (Table 1, group 1) that received composite grafts of nontransfected, B6a myoblasts or Fas-expressing myoblasts together with allogeneic C3H (H-2<sup>k</sup>) islets had a mean survival time (MST) of 10.1 and 7.8 days, respectively, similar to the MST of 10.8 days of control animals that received C3H islet allografts alone. In contrast, transplantation of composite grafts of Bfasl myoblasts (Table 1, group 2) resulted in uniform prolongation of islet allograft

survival with an MST of >84 days for those animals that received the largest number of Bfasl muscle cells. Reducing the number of Bfasl myoblasts cotransplanted with the islet allograft resulted in a decrease in MST, demonstrating dose dependency of protection against rejection.

To ascertain whether the Bfasl myoblasts conferred immunoprotection in a transplant site-specific fashion, we transplanted Bfasl myoblasts and C3H islet allografts separately into contralateral kidneys of B6 recipients. These recipients rejected the islet allograft in the normal manner, with an MST of 10.4 days (Table 1, group 3). To test for immunospecificity, we transplanted Bfasl and C3H islet composite grafts and a third-party A/J (H-2<sup>a</sup>) thyroid allograft separately into the two kidneys of B6 recipients. Histological examination after 10 days revealed almost complete rejection of the thyroid graft (Fig. 2A). In contrast, histology of the contralateral graft revealed the presence of intact islets surrounded by muscle cells (Fig. 2B). Control animals that received B6a myoblast-islet composite grafts showed the complete absence of islet cells 10 days after transplantation (Fig. 2C). The muscle cells in the Bfasl composite graft were positive for FasL expression (Fig. 2D), whereas those in the B6a graft were FasL<sup>-</sup> (Fig. 2E). The infiltrating mononuclear cells in the Bfasl composite graft showed extensive apoptosis (Fig. 2F), as detected by in situ terminal deoxynucleotidyl transferase-catalyzed DNA nick end labeling (TUNEL) (9); infiltrating mono-

**Fig. 1.** Bfasl myoblast expression of FasL and induction of apoptosis in Fas<sup>+</sup> YAC-1 cells. **(A)** FACS analysis of Bfasl myoblasts with the specific counterreceptor Fas-Fc fusion protein. B6a (solid trace) and Bfasl (dotted trace) myoblasts were stained with a 96-hour culture supernatant from Neuro-2a cells (American Type Culture Collection, Rockville, Maryland) that had been transfected with the expression plasmid pFAS-FcII (13) with the use of lipofectamine (4). Binding of the fusion protein was detected by sequential labeling with biotin-conjugated goat antibodies to human immunoglobulin (Fc-specific) and streptavidin-conjugated fluorescein isothiocyanate (Zymed, San Francisco, California). **(B)** Bfasl myoblast-induced death of Fas<sup>+</sup> YAC-1 cells. YAC-1 cells ( $1 \times 10^5$ ) were cocultured with various numbers of Bfasl (open bars) or B6a (shaded bars) myoblasts, as indicated, in 96-well flat-bottom tissue culture plates. After incubation for 12 hours, equal portions of nonadherent cells were removed and percentage cell death was measured with a colorimetric assay as described (14). **(C)** Bfasl myoblast-induced fragmentation of YAC-1 nuclear DNA. YAC-1 cells ( $2 \times 10^6$ ) were cocultured with a confluent monolayer of B6a (lane 2) or Bfasl (lane 3) myoblasts in 35-mm plates for 12 hours. DNA from YAC-1 cells was isolated with a G NOME DNA (BIO 101, La Jolla, California) isolation kit, resolved on a 2% agarose gel, and stained with ethidium bromide. Lane 1, DNA molecular size markers.

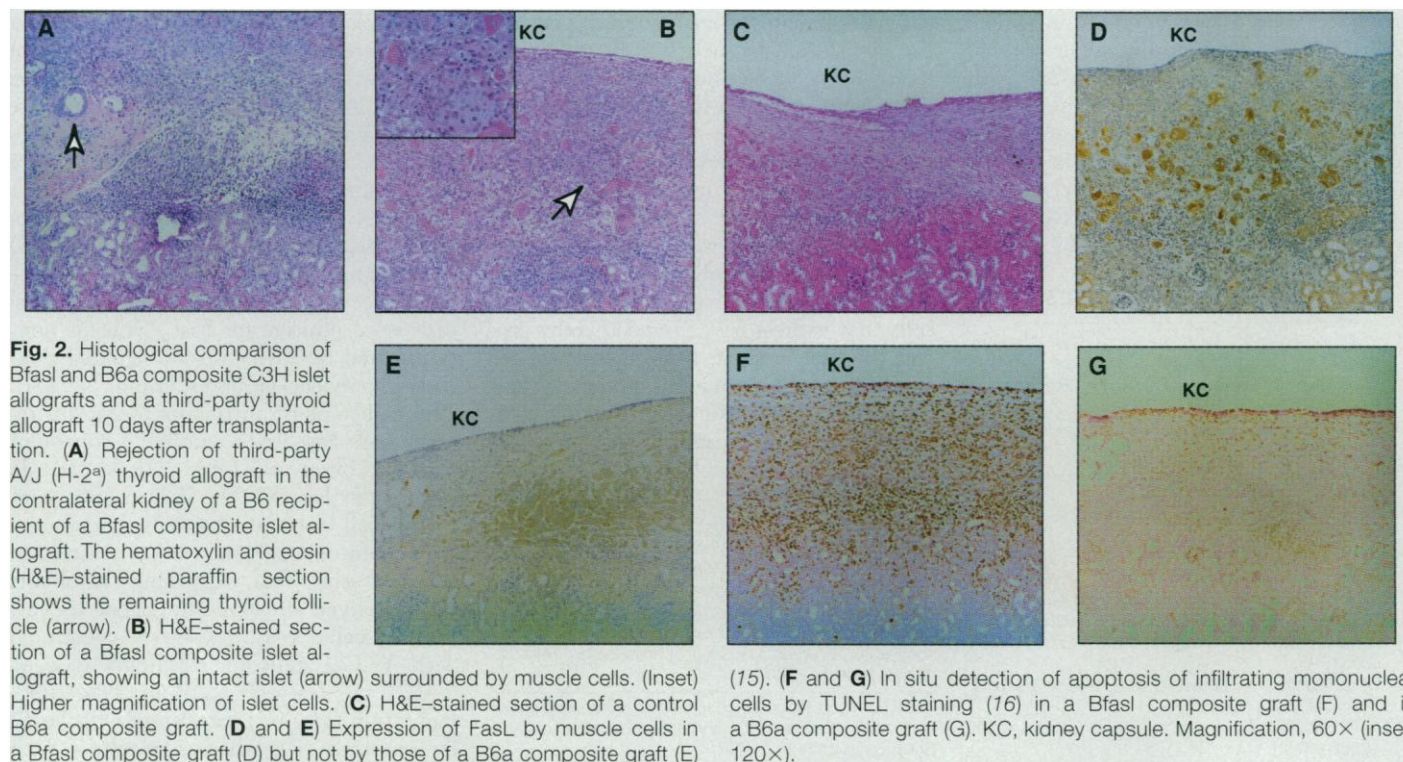
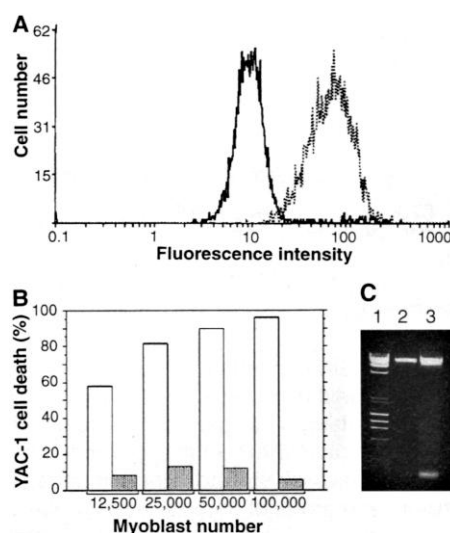


**Fig. 2.** Histological comparison of Bfasl and B6a composite C3H islet allografts and a third-party thyroid allograft 10 days after transplantation. **(A)** Rejection of third-party A/J (H-2<sup>a</sup>) thyroid allograft in the contralateral kidney of a B6 recipient of a Bfasl composite islet allograft. The hematoxylin and eosin (H&E)-stained paraffin section shows the remaining thyroid follicle (arrow). **(B)** H&E-stained section of a Bfasl composite islet allograft, showing an intact islet (arrow) surrounded by muscle cells. (Inset) Higher magnification of islet cells. **(C)** H&E-stained section of a control B6a composite graft. **(D and E)** Expression of FasL by muscle cells in a Bfasl composite graft (D) but not by those of a B6a composite graft (E)

(15). **(F and G)** In situ detection of apoptosis of infiltrating mononuclear cells by TUNEL staining (16) in a Bfasl composite graft (F) and in a B6a composite graft (G). KC, kidney capsule. Magnification, 60 $\times$  (inset, 120 $\times$ ).

nuclear cells in the control B6a graft showed minimal evidence of apoptosis (Fig. 2G).

To confirm that the composite Bfasl myoblast-islet allografts were responsible for maintenance of normoglycemia, we removed the manipulated kidneys of two grafted animals 30 and 44 days after transplantation. The blood glucose concentrations of both animals reverted to pretransplant, hyperglycemic values within 48 hours of nephrectomy (Fig. 3, A and B). In ~25% of the animals that received  $\geq 10^6$  Bfasl myoblasts with their islet allografts, blood glucose concentrations fluctuated within the first 10 days after transplantation (Fig. 3B) and then stabilized at normoglycemic values. Such fluctuation was not observed in animals that received smaller numbers of myoblasts in their composite grafts. Histological examination of the explanted grafts (Fig. 3C) revealed the presence under the kidney capsule of cells containing insulin granules interspersed with multinucleated cells that showed a morphology consistent with that of fused myotubules and which also expressed FasL. All the animals that received composite Bfasl myoblast and islet allografts remained apparently healthy and active. Random evaluation of liver function revealed that serum concentrations of alanine aminotransferase, aspartate aminotransferase, total bilirubin, and  $\alpha$ -glutamyl transpeptidase were within normal limits. In addition, these animals showed normal concentrations of blood urea nitrogen and creatinine, indicat-

ing normal liver and kidney function. In animals that became hyperglycemic after 60 days, histology revealed loss of both islets and FasL expression despite the presence of muscle cells (10).

Our data are consistent with recent demonstrations that FasL expression in the anterior chamber of the eye and testes is responsible in part for the immunoprivileged status of these sites (11). Soluble FasL or monoclonal antibodies to Fas produced systemic toxicity in the form of fulminant hepatic failure in mice (12). However, the animals in our study showed no gross abnormalities and had normal kidney and liver function. The loss of transgene expression after 60 days correlated with rejection of the islet allograft, indicating that continued expression of FasL is necessary for protection against allograft rejection.

We have developed an approach toward facilitation of islet allograft transplantation that relies on syngeneic myoblasts genetically engineered to deliver an apoptotic signal by means of FasL expression. This approach offers an opportunity to manipu-

late the local environment of an islet allograft in composite grafting. The ability of genetically engineered primary myoblasts to differentiate into postmitotic myotubules and to continue to express recombinant protein makes them potentially safe, non-malignant carrier cells for the delivery of FasL or other immunosuppressive molecules. Further investigations will be necessary to elucidate whether such an approach will confer long-term safety and specific immunotolerance.

REFERENCES AND NOTES

1. H. Yagita et al., *Immunol. Rev.* **146**, 223 (1995); P. Golstein, D. Marguet, V. Depraetere, *ibid.*, p. 45; D. H. Lynch, F. Ramsdell, M. R. Alderson, *Immunol. Today* **16**, 570 (1995); S. Nagata, *Adv. Immunol.* **57**, 129 (1994).
2. F. Ramsdell et al., *Int. Immunol.* **6**, 1545 (1994); F. Vignaux et al., *J. Exp. Med.* **181**, 781 (1995).
3. E. Barr and J. Leiden, *Science* **254**, 1507 (1991); J. Dhawan et al., *ibid.*, p. 1509; M. Cantini et al., *In Vitro Cell. Dev. Biol.* **30A**, 131 (1994); T. A. Rando and H. M. Blau, *J. Cell Biol.* **125**, 1275 (1994).
4. Myoblasts were derived from thigh muscles of adult B6 mice 72 hours after treatment with 25  $\mu$ l of 0.25% bupivacaine intramuscularly. Primary cultures were maintained as myoblasts in F10 medium supplemented with 20% (v/v) fetal bovine serum and basic fibroblast growth factor (2.5 ng/ml) (Promega, Madison, WI). Murine FasL or human Fas complementary DNA was cloned into the BCMGS Neo expression plasmid (6), and B6 myoblasts were transfected with 10  $\mu$ g of plasmid DNA and 40  $\mu$ g of lipofectamine (Gibco, Gaithersburg, MD) in 100-mm plates. Selection with G418 (200  $\mu$ g/ml) (Gibco) was initiated 48 hours after transfection and continued for 2 weeks, after which resistant colonies were pooled and designated Bfasl or Bfas.
5. F. Leithauser et al., *Lab. Invest.* **69**, 415 (1993).
6. A. Rensing-Ehl et al., *Eur. J. Immunol.* **25**, 2253 (1995).
7. C. B. Thompson, *Science* **267**, 1456 (1995).
8. B6 mouse (Jackson, Bar Harbor, ME) recipients of islet allografts were rendered diabetic with streptozotocin (250 mg per kilogram of body weight, intraperitoneal) (Upjohn, Kalamazoo, MI). Only animals with blood glucose concentrations of >350 mg/dl (Chemstrip bG; Boehringer Mannheim, Indianapolis, IN) were used as recipients of islet allografts. Islets were obtained from C3H mice (Jackson) by stationary collagenase digestion of the pancreas and Ficoll gradient fractionation. Approximately 300 islets were used per islet-myoblast composite graft and were transplanted under the kidney capsule of ketamine-tranquilized animals (100 mg per kilogram of body weight, intraperitoneally) with a glass capillary pipette in ~25  $\mu$ l of Hanks' balanced salt solution containing 5% (v/v) horse serum. Third-party thyroid allografts comprised 1-mm slices and were placed under the contralateral kidney capsule. Posttransplant blood glucose concentrations were determined three times weekly. After return to normoglycemia (<200 mg/dl), animals with three consecutive blood glucose concentrations of >250 mg/dl were considered to have rejected their islet allograft.
9. Y. Gavrielle, Y. Sherman, S. A. Ben-Sasson, *J. Cell Biol.* **119**, 493 (1992).
10. M. Yu and H. T. Lau, data not shown.
11. D. Bellgrau et al., *Nature* **377**, 630 (1995); T. S. Griffith, T. Brunner, S. M. Fletcher, D. R. Green, T. A. Ferguson, *Science* **270**, 1189 (1995).
12. J. Ogasawara et al., *Nature* **364**, 806 (1993).
13. T. Suda and S. Nagata, *J. Exp. Med.* **179**, 873 (1994).
14. R. A. Miller, in *Current Protocols in Immunology*, J. E. Coligan, A. M. Kruisbeek, D. H. Margulies, Eds. (Wiley, New York, 1993), vol. 1, chap. 3.15.

**Table 1.** Survival of C3H islet allografts in B6 diabetic recipients. In groups 1 and 2, composite myoblast and islet allografts were transplanted under the left kidney capsule. In group 3, the islets and Bfasl myoblasts were transplanted separately under the left and right kidney capsules, respectively.

Myoblasts (number)	Individual survival (days)	MST (days)
<i>Group 1</i>		
None	10, 10, 11, 11, 12	10.8
B6a ( $1 \times 10^6$ )	9, 9, 10, 10, 11, 12	10.1
Bfas ( $1 \times 10^6$ )	6, 7, 8, 8, 10	7.8
<i>Group 2</i>		
Bfasl ( $2 \times 10^6$ )	69, 70, 77, 77, 80, >100, >100, >100	>84.1
Bfasl ( $1 \times 10^6$ )	30,* 44,* 61, 61, 65, 88, >100, >100	>79
Bfasl ( $0.5 \times 10^6$ )	24, 49, 56, 59, 68, 77, 77, 81, 85, 90	66.6
Bfasl ( $1 \times 10^4$ )	15, 15, 15, 41, 41	26
<i>Group 3</i>		
Bfasl ( $1 \times 10^6$ )	10, 10, 10, 10, 12	10.4

\*Allograft-bearing kidneys were removed at the indicated times for histological examination, and the blood glucose concentration of the animals was monitored (Fig. 3).

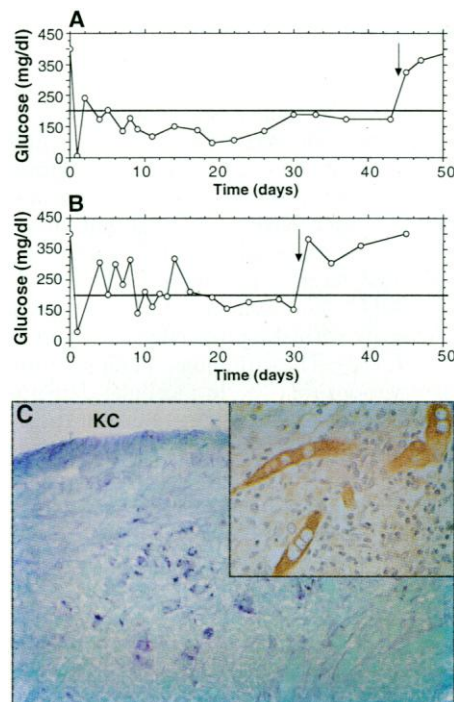


**Fig. 3.** Effects of removal of the kidney bearing composite Bfasl myoblast and C3H islet allografts from B6 recipient mice. (A and B) Blood glucose concentrations at the indicated times after transplantation; arrows indicate nephrectomy performed 44 (A) and 30 (B) days after transplantation. Shaded horizontal line represents the upper limit of normal blood glucose concentrations (80 to 200 mg/dl). (C) Histology of graft 44 days after transplantation stained with aldehyde fuchsin to detect insulin granules. (Inset) Muscle cells stained for FasL (15). Magnification, 100 $\times$  (inset, 200 $\times$ ).

15. Grafts fixed with Bouin's solution were embedded in paraffin, which was subsequently removed from 5- $\mu$ m sections by treatment with xylene. The sections were rehydrated by exposure to a graded series of ethanol solutions, and endogenous peroxidase was quenched with 0.1% H<sub>2</sub>O<sub>2</sub> in phosphate-buffered saline (PBS) for 15 min. Nonspecific sites were blocked with 10% goat serum and 0.3% Triton X-100 in PBS for 1 hour, with addition of free avidin to block endogenous biotin followed by incubation for 30 min with free biotin. The sections were then incubated overnight at 4°C with undiluted culture supernatant from pFAS-Foll-transfected Neuro-2a

cells. Fas-Fc binding was detected by sequential application of biotin-conjugated goat antibodies to human immunoglobulin (Fc specific), streptavidin-conjugated horseradish peroxidase, and diaminobenzidine substrate solution (Zymed, San Francisco, CA). Sections were then counterstained with hematoxylin.

16. Grafts fixed with Bouin's solution were processed for paraffin sectioning. Deparaffinized and rehydrated sections were digested with proteinase K (20  $\mu$ g/ml) for 15 min at room temperature, and endogenous peroxidase activity was quenched with 0.1% H<sub>2</sub>O<sub>2</sub> in PBS for 15 min. Sections were then incubated with

10% goat serum in PBS for 1 hour, after which the 3'-OH ends of fragmented DNA were labeled by TUNEL with an in situ cell death detection kit (Boehringer Mannheim, Mannheim, Germany). Sections were then counterstained with eosin.

17. Care and use of all animals were in accordance with the guidelines of the animal care committee of the Children's Hospital of Philadelphia. We thank J. M. Templeton Jr. for his support; K. High and S. Surrey for critical review of the manuscript; and S. Nagata for reagents.

23 January 1996; accepted 2 May 1996

## Evidence for Physical and Functional Association Between EMB-5 and LIN-12 in *Caenorhabditis elegans*

E. Jane Albert Hubbard, Qu Dong, Iva Greenwald\*

The *Caenorhabditis elegans* LIN-12 and GLP-1 proteins are members of the LIN-12/Notch family of receptors for intercellular signals that specify cell fate. Evidence presented here suggests that the intracellular domains of LIN-12 and GLP-1 interact with the *C. elegans* EMB-5 protein and that the *emb-5* gene functions in the same pathway as the *lin-12* and *glp-1* genes. EMB-5 is similar in sequence to a yeast protein that controls chromatin structure. Hence, a direct consequence of LIN-12 or GLP-1 activation may be an alteration of chromatin structure that produces changes in transcriptional activity.

Transmembrane proteins of the LIN-12/Notch family are found throughout the animal kingdom. The *Caenorhabditis elegans* genes *lin-12* and *glp-1* and the *Drosophila* gene *Notch* were first defined by mutations that alter cell fate decisions involving cell-cell interactions (1-3). In vertebrates, *lin-12/Notch* genes are also involved in cell fate decisions (4). It is now generally accepted that LIN-12/Notch proteins function as receptors that are activated by binding ligands of the Delta/Serrate/LAG-2 family (5). The intracellular domain of LIN-12/Notch proteins, and in particular the region encompassing six CDC10/SW16 (ankyrin) motifs, has the intrinsic signal-transducing activity of the intact protein (6). However, there is no known biochemical activity associated with the intracellular domain of LIN-12/Notch proteins. Understanding the downstream consequences of receptor activation therefore requires the identification and characterization of the interacting components involved in *lin-12/Notch*-mediated cell fate decisions.

E. J. A. Hubbard and Q. Dong, Department of Biochemistry and Molecular Biophysics, Columbia University College of Physicians and Surgeons, New York, NY 10032, USA.

I. Greenwald, Department of Biochemistry and Molecular Biophysics and Howard Hughes Medical Institute, Columbia University College of Physicians and Surgeons, New York, NY 10032, USA.

\*To whom correspondence should be addressed. E-mail: greenwald@cuccfa.ccc.columbia.edu

One such component, named Su(H) in *Drosophila* and LAG-1 in *C. elegans*, is similar to the mammalian CBF1 transcription factor (7, 8). Genetic studies in *Drosophila* and *C. elegans* have established that Su(H) and LAG-1 are involved in LIN-12/Notch-mediated reception of intercellular signals (7, 9-11). Furthermore, Su(H) interacts physically with the intracellular domain of Notch (10). These findings, along with the observations that the intracellular domains of LIN-12/Notch proteins have intrinsic signal-transducing activity and when expressed alone are localized in the nucleus, have led to models proposing that there is no intervening cascade of second messengers involved in signal transduction initiated by LIN-12/Notch activation. Instead, upon receptor activation, the intracellular domain may influence target gene expression by activating a transcription complex, or it may function as part of a transcription complex (5).

To identify potential components involved in LIN-12/Notch signal transduction, we used the yeast two-hybrid screen (12, 13). A plasmid library of fusions between the GAL4 activation domain (GAD) and *C. elegans* cDNA sequences (14) was screened for interaction with a fusion protein containing the Gal4p DNA binding domain (GBD) and the CDC10/SW16 (ankyrin) motifs of LIN-12 (15). Partial-sequence analysis of candidate clones and

subsequent database searches revealed that two clones, E7 and E16, contain different GAD fusions to EMB-5 sequences (Table 1). E7 and E16 also interact to a comparable extent with a fusion protein containing the corresponding region of GLP-1 fused to GBD (Table 1). This result suggests that the interaction is meaningful, because *lin-12* and *glp-1* are functionally and biochemically interchangeable (9, 16). In contrast, E7 and E16 do not interact with the functionally and structurally unrelated proteins laminin (human) and SNF1 (*Saccharomyces cerevisiae*), or with a functionally unrelated *C. elegans* protein FEM-1 that contains CDC10/SW16 motifs (Table 1).

**Table 1.** EMB-5 interacts with LIN-12 and GLP-1 in the yeast two-hybrid system. Yeast strain Y153 (13) was sequentially transformed with (i) a plasmid encoding a fusion protein between the Gal4p DNA binding domain (GBD) and another sequence (DNA binding hybrid) and (ii) a plasmid encoding a fusion protein between the Gal4p activation domain (GAD) and another sequence (activation hybrid). A blue colony color in the filter assay indicates that  $\beta$ -galactosidase ( $\beta$ -Gal) activity is present, implying a physical association between the DNA binding and activation domain hybrids as a result of inserted sequences. nd, not done.

DNA binding hybrid*	Activation hybrid†	Colony color	$\beta$ -Gal activity (Miller units)‡
LIN-12	EMB-5	Blue	4.7 $\pm$ 0.6
GLP-1	EMB-5	Blue	5.3 $\pm$ 0.2
LIN-12	SNF4	White	0.8 $\pm$ 0.6
GLP-1	SNF4	White	0.4 $\pm$ 0.1
SNF1	EMB-5	White	0.6 $\pm$ 0.1
Lamin	EMB-5	White	nd
FEM-1	EMB-5	White	nd
SNF1	SNF4	Blue	28.5 $\pm$ 4.5

\*DNA binding hybrids in the pAS1 vector (13) contain sequences fused to GAL4p(1-147). LIN-12 = pASL2, containing LIN-12(940-1320). GLP-1 = pASG2, containing GLP-1(867-1171). pAS-SNF1 was derived from pEE5 (12). pAS-FEM-1 encodes a hybrid containing the CDC10-SW16 motifs of FEM-1 (26). †EMB-5 activation domain hybrids in the pACT vector contain sequences fused to GAL4p(768-881) (13). For EMB-5, the data are from the E7 clone, which contains EMB-5(894-1521). Similar results were obtained for the E16 clone, which contains EMB-5(835-1521) (27). The SNF4 clone was pNI12 (12). ‡Miller units are described in (28). The standard deviation is indicated. Each value is the average of four transformants.